

Rigid backbone polymers. Dielectric relaxation of isotropic and lyotropic solutions of a copolymer of n-butyl isocyanate and n-nonyl isocyanate

J. K. Moscicki* and G. Williams

Edward Davies Chemical Laboratories, University College of Wales, Aberystwyth, SY23 1NE, UK

and S. M. Aharoni

Allied Chemical Corporation, Morristown, N.J., 07960, USA

Received 16 March 1981; revised 3 June 1981)

The dielectric relaxation behaviour of solutions of a copolymer of n-butyl and n-nonyl isocyanate in toluene has been studied over a range of concentration extending from the isotropic to the lyotropic solution states. A marked decrease in relaxation magnitude on going from the isotropic to lyotropic state is attributed to a restriction of angular motions to a 'virtual-cone', thus giving only a partial relaxation of the mean square dipole moment of the chains. The models of restricted motion due to Warchol and Vaughan and to Wang and Pecora are applied to the data and it is suggested that the chains move in the lyotropic phase through rather larger angles than would be expected in a rigid cone of solid angle, this being allowed by a combination of the movement of the surrounding chains and through angular fluctuations in the local director.

INTRODUCTION

The mesomorphic behaviour of different rigid-backbone poly(alkylisocyanates) has been described by Aharoni and co-workers¹⁻⁹. A homologous series of poly(n-alkyl isocyanates) (PnAIC say) was studied in bulk and in solution. It was found that for the bulk polymers the middle members of the series, with side alkyl chain length in the range $4 \leq m < 13$ (where m is the number of carbon atoms), exhibit a thermotropic mesomorphic phase at temperatures above 100°C. Unfortunately a gradual decomposition, which sets in at about 120°C and accelerates at about 140°C, does not allow dielectric studies of mesophases of the bulk materials to be carried out. The same homologous series studied as highly concentrated solutions exhibits lyotropic mesomorphic behaviour for $4 \leq m < 13$. Whilst thermal decomposition occurs for such solutions it is not a critical factor in the study of the physical behaviour of the isotropic and lyotropic solutions. Preliminary investigations by Aharoni and co-workers established the important facts about the solution properties of different PnAIC. First of all, the phase transition from the isotropic phase to nematic phase with increasing polymer concentration is not sharp. There exists a range where isotropic and nematic phases coexist, called the biphasic range, where a continuous increase in the ratio of the amount of nematic to lyotropic material occurs as polymer concentration is increased. Secondly, measurements of flow viscosity η as a function of polymer concentration showed that η passed

through a maximum at a critical concentration of polymer. This maximum appears not at the concentration where the anisotropic phase is first observed in polarized optical microscopy studies of the material but is substantially within the bi-phasic range.

Since PnAIC molecules are helical and rod-like having their dipole moment vectors lying along the long axis of the molecule¹⁵, it is expected that dielectric studies of the isotropic and lyotropic phases would yield useful information on their structure and dynamics. Dielectric studies in the isotropic phase at small polymer concentrations have been made for butyl, hexyl and octyl isocyanate polymers by Yu *et al.*¹⁰, Bur and Roberts¹¹, Dev *et al.*¹², Pierre and Marchal¹³, Bur and Fetters^{14,15}, Beevers *et al.*¹⁶ and by Coles *et al.*¹⁷. The latter studies^{16,17} also investigated the static and dynamic Kerr-effect behaviour of the solutions. The conclusions of these studies are that in dilute solution the molecules behave as rigid-rods at low molecular weight but above a molecular weight $\sim 10^5$ they deviate from rods, forming rather stiff coils at the highest molecular weights. In addition angular motion occurs as a simple small-step rotational diffusion process for dilute solutions of the rod-like molecules and since the materials studied always have a distribution of molecular weight, the dielectric loss curves and the Kerr-effect transients are far broader than those for a single relaxation time process. It was shown¹⁰⁻¹⁷ that increase of temperature increased the tendency of the chains to deviate from the rigid-rod conformation, this being especially apparent from the marked decrease^{16,17} in mean square dipole moment $\langle \mu^2 \rangle$ and static Kerr-constant K_s with increasing

* Permanent address: Institute of Physics, Jagellonian University, ul Reymonta 4, 30-059 Krakow, Poland

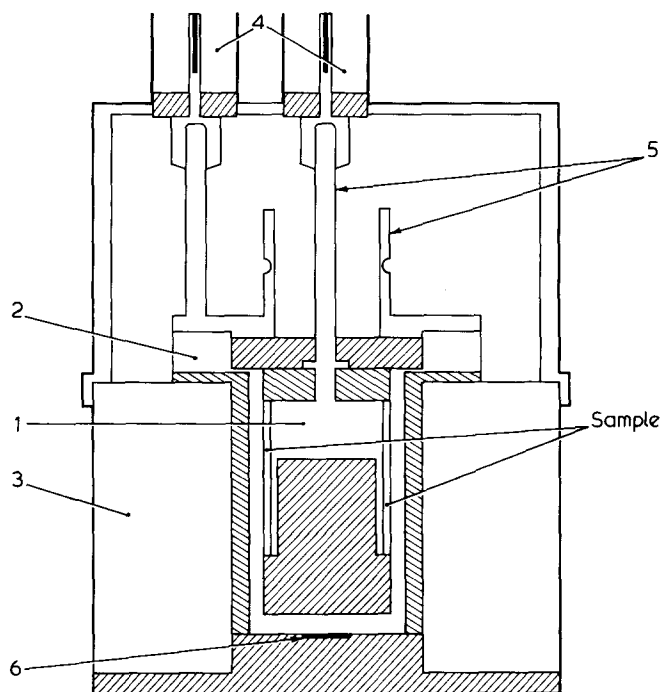


Figure 1 The dielectric cell: for a description see text

temperature. At only moderate concentrations there was evidence¹⁷ for aggregation of poly(*n*-hexyl isocyanate) molecules in toluene solution.

The present work reports our dielectric studies of a copolymer of *n*-butyl and *n*-nonyl isocyanates over a range of concentration extending up to 40% (w/w) of polymer in solution in toluene, and over a limited range of temperature.

EXPERIMENTAL

The sample of copolymer made from 50% *n*-butyl and 50% *n*-nonyl isocyanates was one of those prepared by Aharoni and described earlier¹. It had a reduced viscosity at $C = 0.5\%$ of 2.4 in chloroform which gives¹⁵ a molecular weight, $M_w = 87000$. Seven different solutions: 5, 10.1, 15.3, 18.6, 26.4, 35.0 and 40.0% polymer (w/w) in toluene covering isotropic and mesomorphic phases at room temperatures were investigated. The toluene was of AR grade and was dried over zeolite before use. Solutions were made by shaking the polymer/solvent mixture for several hours followed by centrifugation to deposit particulate matter and to eliminate air bubbles. Owing to the high evaporation rate of toluene and the high viscosity of the most concentrated solutions the specially-designed cell shown in Figure 1 was constructed. The polymer solution sits between the low-potential (1) and high-potential (2) electrodes. The assembly is electrically insulated (teflon) from the thermostatically-controlled jacket (3) (maintained at earth potential) through which a circulating liquid (alcohol or water) is passed. The assembly (1), (2) can be bodily removed and placed in a centrifuge. The connections may be two-terminal (5, a G.R. connector) or three-terminal (4), where, for the latter, we have high, low and guard (=earth) as the three terminals. Temperatures were controlled to $\pm 0.1^\circ\text{C}$ with the aid of a thermosensor (6). The empty cell had a capacitance of about 6 pF and this was reproducible to 0.3% following the dismantling and reassembling operations required for emptying and filling the cell. Dielectric measurements of PBNIC were made using a

three-terminal arrangement and employed a Sullivan C306D Transformer Bridge (60 Hz to 10^5 Hz and a Scheiber Bridge (10^{-2} to 3×10^2 Hz)). Agreement within 1% was obtained for the complex permittivity ($\epsilon = \epsilon' - i\epsilon''$) when measured by both bridges in their range of overlap.

With regard to the processing of dielectric data, all solutions exhibited marked conductivity effects at the lowest frequencies. Figures 2 and 3 show the loss-factor (ϵ'') and relative permittivity (ϵ') as a function of frequency for PBNIC solutions at 24°C . The rapid increase in ϵ'' at the lowest frequencies arises due to conductivity of the solutions, (note the logarithmic scale in Figure 2 and also the large magnitude of ϵ' and ϵ''). In the presence of d.c.

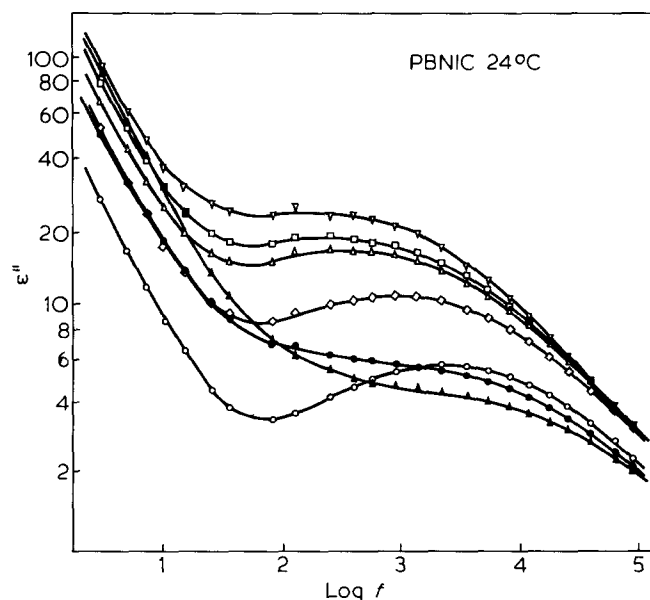


Figure 2 Dielectric loss-factor $\epsilon''(f)$ for PBNIC/toluene solutions at 24°C . $\circ, \diamond, \triangle, \square, \nabla, \bullet$ and \blacktriangle correspond to 5.0, 10.1, 15.3, 18.6, 26.4, 35.0 and 40% (w/w) polymer respectively

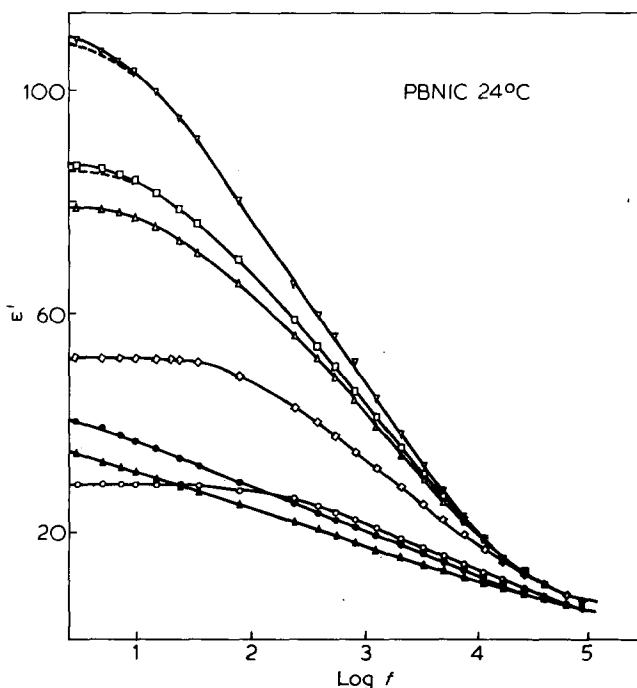


Figure 3 Dielectric permittivity $\epsilon'(f)$ for PBNIC/toluene solutions at 24°C . Symbols as for Figure 2 for different concentrations of polymer

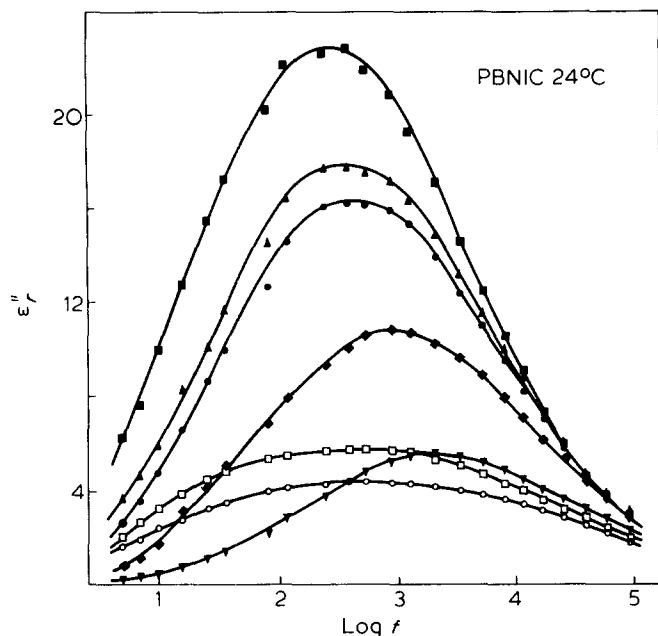


Figure 4 $\epsilon''(f)$ for PBNIC/toluene solutions at 24°C. ∇ , \diamond , \bullet , \triangle , \blacksquare , \square , and \circ correspond to 5.0, 10.1, 15.3, 18.6, 26.4, 35.0 and 40% (w/w) polymer respectively

conductance the total loss-factor may be written as:

$$\epsilon'' = \epsilon''_r + \epsilon''_c = \epsilon + \frac{3.6\pi\sigma}{\omega} \times 10^{12} \quad (1)$$

where ϵ''_r is due to relaxation and ϵ''_c is due to d.c. conductivity. σ and ω ($= 2\pi f/\text{Hz}$) are specific conductivity (in $\text{ohm}^{-1} \text{cm}^{-1}$) and angular frequency respectively. A d.c. conductivity may lead to electrode polarization and hence to a difference between the observed permittivity and the 'intrinsic' permittivity ϵ'_r of the material. The difference is a function of frequency and has a form²¹:

$$\epsilon' - \epsilon'_r = \frac{\delta}{f^2} \quad (2)$$

Using the usual expressions for dielectric dispersion (see e.g. ref. 18) we may expand ϵ'_r and ϵ''_r as power series in f^n , so with equations (1) and (2) we obtain:

$$\epsilon'.f^2 = \delta + \epsilon_\infty f^2 + a_1 f^3 + a_2 f^4 + \dots \quad (3a)$$

$$\epsilon''.f = \sigma + b_1 f^2 + b_2 f^3 + \dots \quad (3b)$$

Here ϵ_∞ is the limiting high frequency permittivity.

Our data from Figures 2 and 3, in the low frequency region with respect to the loss peaks were fitted by a least squares procedure allowing δ and σ to be determined and hence allowing ϵ'_r and ϵ''_r to be evaluated at each frequency with the aid of equations 2 and 1 respectively.

In Figure 3 the broken lines correspond to the corrected permittivities and Figure 4 shows the loss-curves corrected for low-frequency conductivity effects.

RESULTS

The permittivity and loss curves of Figures 3 and 4 contain information on the variation of (i) the magnitude, (ii) the location and (iii) the shape of the loss-process with polymer concentration. The qualitative features are as follows. Increasing the concentration of polymer from 5%

to 26.4% gives an increased size of loss peak, a decrease in the frequency of maximum loss (f_m), but little change in the shape of the loss curve. Further increase in concentration to 35% and 40% results in a dramatic decrease in the magnitude of the loss-peak, ϵ''_{rm} , and the dielectric increment ($\epsilon_{ro} - \epsilon_\infty$), a shift of $\log f_m$ to higher frequencies and a considerable broadening of the relaxation curve compared with that found for lower concentrations. Up to about 15% polymer, these solutions are isotropic but at the higher concentrations studied here they form the lyotropic-nematic mesophase, as is evidenced by their turbidity and by the observations of characteristic structures in the polarizing microscope. Figure 5 shows the Cole-Cole (or Argand) diagrams for the relaxation in a nematic and an isotropic solution. For the isotropic solution the curve resembles that of Davidson-Cole function whilst that for the nematic solution resembles that for a Cole-Cole function (see e.g. ref. 18). Figure 6 summarizes the variation of $\log f_m$, ϵ''_{rm} , $\log \sigma$ and ϵ_{ro} with concentration for the two temperatures studied.

DISCUSSION

For the isotropic solutions the dielectric relaxation is qualitatively similar to that found for different PnAIC by earlier studies¹⁰⁻¹⁷. Those studies had shown that the molecules reorientate by small-step rotational diffusion, that the persistence-length of the rod-like chain decreases with increasing temperature and that the shape of the observed loss-peak is very sensitive to a molecular weight distribution (see Bur and Roberts¹¹ and Beevers *et al.*¹⁶). The same conclusions apply to our data for dilute solutions of PBNIC in the isotropic liquid state. We have reported earlier for a poly(n-hexyl isocyanate)/toluene system¹⁹ that ϵ''_{rm} increased linearly with c up to 15% polymer. Our present results, Figure 6b, show that ϵ''_{rm} increases linearly with c up to about 15% but a downward curvature is obtained for higher concentrations in the isotropic range. Similar observations apply to Figure 6d. We note that $\log f_m$ decreases approximately linearly with c for $c < 15\%$ (see Figure 6a) then deviates upwards. The linear increases in ϵ''_{rm} and ϵ_{ro} suggest that no extensive

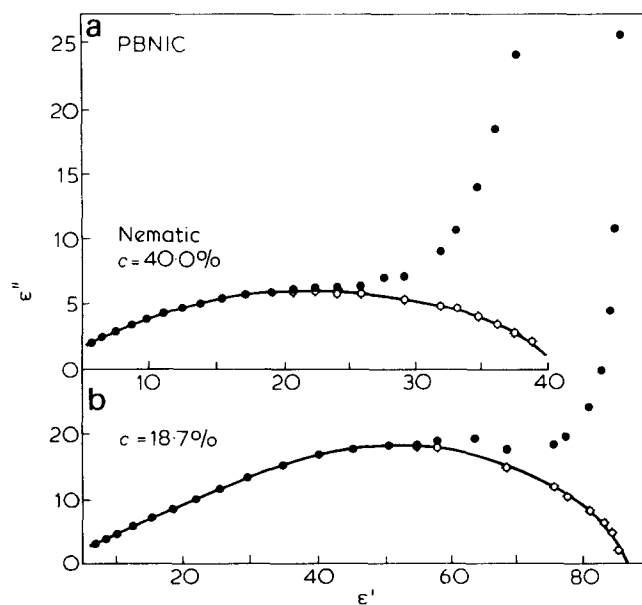


Figure 5 Argand diagram for (a) $C = 40\%$ and (b) $C = 18.7\%$ PBNIC in toluene at 24°C

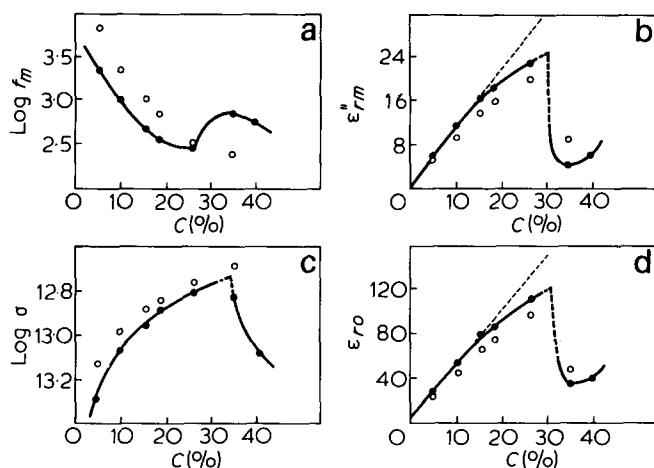


Figure 6 (a) $\log(f_m/\text{Hz})$ (b) ϵ''_{rm} , (c) $\log(\sigma/\text{ohm}^{-1}\text{cm}^{-1})$ and (d) ϵ'_{ro} as a function of polymer concentration c (% w/w) for PBNIC/toluene solutions. \circ , 40°C; \bullet , 24°C

equilibrium angular correlations occur between the molecules in the range up to 15% polymer but since $\log f_m$ is continuously (and linearly) decreasing, that the angular motions of individual molecules are increasingly hindered by the obstructive contacts (or 'dynamic interactions') with the surrounding molecules. For the concentration range above 15% the fall-off in ϵ''_{rm} and ϵ'_{ro} from the linear increase suggests that equilibrium angular correlations are developing rapidly.

This is substantiated by the rapid deviation of $\log f_m$ from its previous linear behaviour. Note that $\log f_m$ deviates to higher frequencies from the linear relation, in the region where equilibrium structures are developing. At first sight we might have thought that as the structures develop the reorientation rate of a reference molecule would become increasingly hindered and consequently that $\log f_m$ would deviate to lower frequencies away from the linear relation. We shall consider this further below.

For $c \leq 26.4\%$ polymer, the loss curves are all asymmetric, in the Davidson-Cole sense, with a half-width of ~ 2.5 units of $\log_{10} f$. In this range the loss-curves are dominated by the contribution from the isotropic phase. Figure 5 shows, as one example, the Argand diagrams for solutions below and above $c = 26.4\%$. The breadth and asymmetry for the curve for $c = 18.7\%$ is to be interpreted in terms of the distribution of molecular weight, and, since the mean-square dipole moment $\langle \mu^2(M) \rangle$ depends strongly upon molecular weight, the loss curves favour the higher molecular weight species in the distribution. An analysis of such curves has been given by Bur and Roberts¹¹ and Beevers *et al.*¹⁶ and will not be discussed here except to say that the high frequency tail is almost certainly dominated by contributions from the lower molecular-weight species. In contrast the Argand diagram for $c = 40\%$ shown in Figure 5 is very broad and nearly symmetrical, and could be approximately fitted using a Cole-Cole empirical relaxation function.

The relaxation behaviour changes dramatically on going from the isotropic to lyotropic states. As shown in Figures 6b and 6d, ϵ''_{rm} and ϵ'_{ro} decrease remarkably on entering the mesophase. This implies that whereas in the dilute isotropic solutions individual molecules may reorientate into 4π solid angle relaxing all of $\langle \mu^2 \rangle$, in the mesophase the nematic potential prevents the molecule from freely reorientating and restricts its motion to a limited solid angle. Motion of this kind will not relax all of

$\langle \mu^2 \rangle$. Complementary to the fall in ϵ''_{rm} and ϵ'_{ro} is the increase in $\log f_m$ and increased broadening of the loss curve (see also Figure 5). An explanation of molecular reorientation of small molecules in the nematic phase is due to Martin *et al.*²⁰. They consider the orientation of the components of dipole vector $\mu_{||}$ associated with the long axis of a molecule in the presence of a nematic potential, $V(\theta)$. Using a form for $V(\theta)$ which allows the dipole vector to point in either direction along the director and assuming the molecule moves in accord with a rotational diffusion equation in which the nematic potential $V(\theta)$ is included, relations were derived between the relaxation times for the randomization of $\mu_{||}$ and the parameters of the model: *viz.* $V(\theta = \pi/2)$ and D_R the diffusion coefficient for free reorientation. In general, all of $\mu_{||}^2$ is relaxed in this model by two mechanisms (1) 'slow' end-over-end reorientation of the molecules over the barrier imposed by the nematic potential (2) 'fast' small angle fluctuations within the two-fold minima of the nematic potential. So, in the absence of directional angular correlations* between a reference dipolar molecule and its neighbours in the nematic phase, the magnitude of loss in the nematic phase would approximate to that extrapolated for isotropic solution. Whilst it is possible that the dipoles of our polymer chains might prefer an antiparallel alignment in the lyotropic phase, leading to a Kirkwood g -factor less than unity, and hence to relatively smaller values of ϵ''_{rm} and ϵ'_{ro} , we consider that end-over reorientation would not be possible due to the length of the polymer chains. Consequently $\mu_{||}^2$ cannot be fully relaxed, in contrast to small molecule liquid crystals (e.g. MBBA, HCB), and we seek a model for partial reorientation based on the restricted motions of the dipoles in the lyotropic phase. We note that the concept of 'partial' and 'total' reorientation has been previously used²³ to give a unified explanation of α , β and $(\alpha\beta)$ relaxations in amorphous polymers, supercooled liquids and molecular glasses.

If the rod-like chains are constrained to move in the limited solid angle of a cone then the magnitude of the process is proportional to $[\langle \mu^2 \rangle - \langle \mu \rangle^2] = \langle \mu^2 \rangle$. G , say, where $\langle \mu^2 \rangle$ is the mean square dipole moment of the free chain and $\langle \mu \rangle$ is the mean dipole moment residing in the cone after partial randomization of the dipole vector. Making the assumption that the vector is free to move in range $0 \leq \theta \leq \theta_0$, where θ is the polar angle for orientation, but is not allowed outside this range, and where $\theta_0 = 0$ coincides with the z -axis (C_∞ -axis) of the cone, then

$$\langle \mu \rangle = \frac{\int_0^{\theta_0} \cos \theta \sin \theta d\theta}{\int_0^{\theta_0} \sin \theta d\theta} = \frac{n \mu_{||} (1 + \cos \theta_0)}{2} \quad (4)$$

n is a unit vector along the z -axis and $|\mu| = \mu_{||}$ in our case. If we define a ratio $G(c)$ to be

$$G(c) = \frac{(\epsilon_{ro} - \epsilon_\infty)_{\text{lyotropic}}}{(\epsilon_{ro} - \epsilon_\infty)_{\text{isotropic}}} \quad (5)$$

where $(\epsilon_{ro} - \epsilon_\infty)_{\text{lyotropic}}$ is the relaxation magnitude in the lyotropic solution at a given polymer concentration c and

* These correlations lead to a Kirkwood-Frohlich g -factor which may differ from unity and, since $(\epsilon_{ro} - \epsilon_\infty)$ is proportional to $g\mu^2$ will affect the magnitude of the total relaxation (e.g. see refs. 18, 22)

$(\varepsilon_{ro} - \varepsilon_{\infty})_{\text{isotropic}}$ is the value of the relaxation magnitude the isotropic solution would have had at c and is obtained from a linear extrapolation of the isotropic solution data of Figure 6d. $(\varepsilon_{ro} - \varepsilon_{\infty})_{\text{isotropic}}$ is the relaxation magnitude for a solution in which the dipoles reorientate into 4π solid angle and $(\varepsilon_{ro} - \varepsilon_{\infty})_{\text{lyotropic}}$ is the relaxation magnitude for the lyotropic solution in which only limited angular motions are allowed. Using the model which leads to equation 4 we may show that

$$\cos \theta_0(c) = 2[1 - G(c)]^{1/2} - 1 \quad (6)$$

For the lyotropic solutions at 35% and 40% polymer concentration we estimate $G = 0.17 \pm 0.02$ so from equation (6) we calculate $\theta_0 = 35^\circ \pm 7^\circ$. This is only a rough estimate since we have not taken account of the molecular weight distribution. If we take the primitive model of the structure of the lyotropic-nematic phase to be that of cylindrical rods of radius r constrained to infinite tubes (created by adjacent rods) then the rotation of the rod about its centre of gravity is allowed to occur up to a maximum angle θ_0 given by $\tan \theta_0 = (2r'/l)$ where l is the length of the rod and r is the effective arc through which the rod is allowed to move. Thus θ_0 decreases with increasing molecular weight (M) of the polymer. This leads to

$$G(c) = \frac{\int P(M) \langle \mu^2(M) \rangle G(M) dM}{\int P(M) \langle \mu^2(M) \rangle dM} \quad (7)$$

where $P(M)$ is the distribution function for molecular weight and $G(M)$ is given by

$$G(M) = 1 - \left[\frac{1 + \cos \theta_0(M)}{2} \right]^2 \quad (8)$$

The restriction of angular motion of a chain of molecular weight M to a cone of polar angle $\theta_0(M)$ for all M clearly leads to $G(c) < 1$ but the behaviour of $\langle \mu^2(M) \rangle \cdot G(M)$ is complicated. $\langle \mu^2(M) \rangle$ increases rapidly with increasing M for alkyl isocyanate polymers¹¹, but $G(M)$ will decrease rapidly with increasing M due to the condition $\tan \theta_0(M) = (2r'M_0/l_0M)$, where M_0 and l_0 are effective mass and length of a repeat unit of the chain. We calculate $G = 0.36$, $\theta_0 = 54^\circ$ and $G = 0.16$, $\theta_0 = 35^\circ$ and $G = 0.06$, $\theta_0 = 20^\circ$ for $0.5M$, M and $2M$, relative to our above calculation for the lyotropic phase. This leads to $\langle \mu^2(M) \rangle \cdot G(M)$ in the ratio 0.09:0.17:0.24 for $0.5M$, M and $2M$ respectively being the relative contributions to the relaxation magnitude for restricted motion and which may be compared with 0.25:1:4 for $0.5M$, M and $2M$ respectively for the isotropic solution. This would imply a preferred contribution to relaxation strength from lower molecular weight species in the mesophase when compared with the contributions for the isotropic solution. This has importance for the frequency location and shape of the loss process in the lyotropic phase, and will be considered below. The above discussion of the equilibrium behaviour has not required a specific model for the restricted motions of chains. The model of Warchol and Vaughan²⁴, of small-step diffusion of a rod in a cone, which was initially developed for dielectric relaxation in glassy matrices, seems an appropriate model for motion of PBNIC in isotropic and lyotropic solutions. Their model has been recently further considered and extended to include dynamic light-scattering and fluorescence depolarization behaviour by Wang and

Pecora²⁵. Ouaho and Pecora^{26,27} have applied this model to rotational motions in flexible polymer/solvent systems, as observed by dynamic light-scattering techniques.

For dielectric relaxation the appropriate correlation function is $\langle \mu(0) \cdot \mu(t) \rangle$ the dipole moment vector correlation function, since the complex permittivity is related to this quantity via a Fourier transformation (see e.g. refs. 22, 23, 28, 29). Warchol and Vaughan²³ and Wang and Pecora²⁵ obtain

$$\langle \mu(0) \cdot \mu(t) \rangle \mu^2 \{ D_1^0 + D_2^0 \exp[-v_2^0(v_2^0 + 1)D_R t] + D_1^1 \exp[-v_1^1(v_1^1 + 1)D_R t] \} \quad (9)$$

D_R is the rotational diffusion coefficient, $D_1^0 = [(1 + \cos \theta_0)/2]^2 = \langle \mu^2 \rangle$ (see equation 4) and represents that part of $\langle \mu^2 \rangle$ which cannot be relaxed since the motion is restricted to a cone. $D_2^0 = 1/12[1 - \cos \theta_0]^2$ and $D_1^1 = 1/3[2 - \cos \theta_0 - \cos^2 \theta_0]$. For $\theta_0 \leq 60^\circ$, D_2^0 is small compared with D_1^0 and D_1^1 so $\langle \mu(0) \cdot \mu(t) \rangle$ consists of a single exponential decay, with relaxation time $[v_1^1(v_1^1 + 1)D_R]^{-1}$, to a constant value D_1^0 . Wang and Pecora give curves of $v_n^m(\theta_0)$ and it is seen that $v_1^1(\theta_0)$ increases only gradually from unity at $\theta_0 = \pi/2$ to about 3 at $\theta_0 = 30^\circ$ then increases markedly giving $v_1^1(\theta_0) = 10$ for $\theta_0 = 10^\circ$, $v_1^1(\theta_0) = 28$ for $\theta_0 = 5^\circ$. Thus as the extent of the motion decreases (θ_0 decreasing) the process of partial relaxation increases in its rate, as expected in physical terms. We had interpreted the decrease in relaxation magnitude (an equilibrium or time-averaged quantity) on going from isotropic solution to lyotropic solution in terms of the restricted motion of chains so if that is correct, equation (9) predicts the $\log f_m$ would show a corresponding increase. Figure 6a shows this to be the case, at least in qualitative accord with the model, since $\log f_m$ (lyotropic) = $\log f_m$ (isotropic) + X where X is 0.8 to 1.1, and we deduce f_m (isotropic) by extrapolation of the dilute isotropic solution values into the lyotropic range. Quantitative interpretations require a knowledge of the dependencies of $\tau(M)$ and $\langle \mu^2(M) \rangle$ upon molecular weight and the form of the distribution of molecular weight, $P(M)$. Some insight may be obtained from Figure 7 where we show a set of schematic diagrams indicating how the overall loss curves arise for the isotropic solution and for the case of restricted angular motion. Whilst $\langle \mu^2(M) \rangle$ and $\tau(M)$ increase with M , the constraint of limited angular motion leads to a considerable modification, as indicated, and hence to a reduction in magnitude and shift to higher frequencies of the overall loss curve. The evidence from light-scattering studies and related studies¹⁵ suggest that the persistence length of PAIC is comparable with molecular length for our sample. An approximate calculation based on cubic and hexagonal close-packing of rods of radius ' r ' yields an inter-rod spacing in the range 1.0 to 1.5 r for a 35% solution. For chains of length in the range 300 to 700 Å and $r = 10$ Å we calculate θ_0 in the range 2° to 7° so that the relaxation strength in the lyotropic solution would be 0.2 to 0.8% of that for the isotropic phase at the given concentration. The experimental values are close to 17% (=100G). This discrepancy could be rationalized by saying that the 'rigid-cone' approximation should be removed so that the chains around the reference chain, which are moving, on average, to the same extent as the reference chain, allow θ_0 to be about double the values given above but this would still give losses lower than those observed, (calculated average angles being

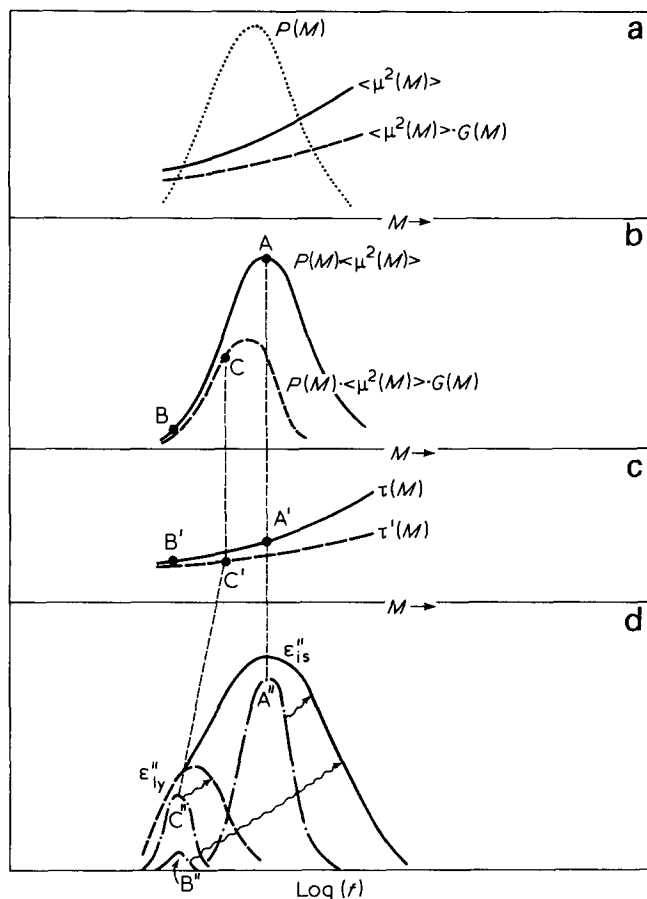


Figure 7 Schematic diagram illustrating the modification of the loss curve for an isotropic solution on going to the lyotropic solution for which angular motions are limited. (a) $P(M)$, $\langle \mu^2(M) \rangle$ and $\langle \mu^2(M) \rangle G(M)$ as a function of molecular weight. As M increases, the effective mean square dipole moment for the restricted motions, $\langle \mu^2(M) \rangle G(M)$ falls increasingly below that for unrestricted motion. (b) $P(M)$, $\langle \mu^2(M) \rangle$ and $P(M) \langle \mu^2(M) \rangle G(M)$ being, respectively, the contributions to the dielectric absorption for isotropic case and for the restricted case from molecular weights in the range M to $M + dM$. (c) $\tau(M)$ and $\tau'(M)$ being, respectively, the relaxation times for the reorientation of a rod in the isotropic case and for the restricted case. As M increases $\tau'(M)$ falls increasingly below $\tau(M)$. (d) Contributions to total loss curves ϵ''_{is} and ϵ''_{ly} from components of the distribution of molecular weight. Contributions from species around A (and A') and B (and B') lead to loss-peaks A'' and B'' for the isotropic case. Contributions from species around C (and C') lead to the loss-peak C''. Thus the overall effect of restricted motion is to reduce the size of the total loss curve and move it to higher frequencies

considerably less than the 35° quoted above) and a frequency shift of loss maximum less than that observed. In view of these results and in view of the prediction of Flory regarding the separation of a polydisperse solution into isotropic and anisotropic phases (see ref. 1 for a further discussion) we are led to the following picture of the lyotropic solutions studied here. First we note that the lyotropic solutions of PBNIC gave optically uniaxial textures, when observed in the polarizing optical microscope. A small fraction of an isotropic-phase inclusion was observed. This isotropic material is presumably saturated isotropic solution and, allowing for polydispersity effects that would preferentially partition lower molecular weight material into the isotropic phase, the reorientational motions in the isotropic inclusions would contribute to the total loss in the region of f_m . However, our calculations suggest that this isotropic material would account for only a small part of the total loss magnitude in the lyotropic solution, so we are led to

conclude that the chains in the wholly lyotropic phase do make the major contribution to the observed loss. It is possible that in that phase there is a tendency for certain regions to be rich in low molecular weight material while other regions are rich in high molecular weight material, giving motion in a range of nematic environments and all substantially contributing to the loss due to the competing factors of $\langle \mu^2(M) \rangle$, $\tau(M)$ and $G(M)$. As a result, extensive angular motions are possible for low molecular weight chains but are severely limited for high molecular weight chains. We suggest that these limited motions occur in a 'virtual-cone' prescribed by the neighbouring chains and that, in addition, angular fluctuations in the local director itself allow the dipole vectors to span a larger solid angle than those calculated above leading to a relaxation magnitude comparable with that being observed in the lyotropic solutions.

In view of the remarkable changes of dielectric behaviour on going from isotropic to lyotropic solutions, further studies are intended on other poly(alkyl isocyanates) in concentrated solution. It is hoped that these studies will include measurements for narrowly fractionated materials.

ACKNOWLEDGEMENTS

The authors gratefully acknowledge the support of the S.R.C. for this work.

REFERENCES

- Aharoni, S. M. *Macromolecules* 1979, **12**, 94
- Aharoni, S. M. and Walsh, E. K. *J. Polym. Sci. Polym. Lett. Edn.* 1979, **17**, 321
- Aharoni, S. M. and Walsh, E. K. *Macromolecules* 1979, **12**, 271
- Aharoni, S. M. *Ferroelectrics* 1980, **30**, 227
- Aharoni, S. M. *Polymer* 1980, **21**, 21
- Aharoni, S. M. and Sibilia, J. P. 20th Canadian High Polymer Forum, August, 1979
- Aharoni, S. M. *Polym. Prepr. Am. Chem. Soc., Div. Polym. Chem.* 1980, **21**(1), 209
- Aharoni, S. M. *J. Polym. Sci. Polym. Phys. Edn.* 1980, **18**, 1303
- Aharoni, S. M. *J. Polym. Sci. Polym. Phys. Edn.* 1980, **18**, 1439
- Yu, H., Bur, A. J. and Fetters, L. J. *Chem. Phys.* 1966, **4**, 2568
- Bur, A. J. and Roberts, D. E. *J. Chem. Phys.* 1969, **51**, 406
- Dev, S. B., Lochead, R. Y. and North, A. M. *Disc. Faraday Soc.* 1970, **49**, 244
- Pierre, J. and Marchal, E. *J. Polym. Sci. Polym. Lett. Edn.* 1975, **13**, 11
- Bur, A. J. and Fetters, L. J. *Macromolecules* 1973, **6**, 874
- Bur, A. J. and Fetters, L. J. *Chem. Rev.* 1976, **76**, 727
- Bevers, M. S., Garrington, D. C. and Williams, G. *Polymer* 1977, **18**, 540
- Coles, H. J., Gupta, A. K. and Marchal, E. *Macromolecules* 1977, **10**, 182
- McCrum, N. G., Read, B. E. and Williams, G. 'Anelastic and Dielectric Effects in Polymeric Solids', J. Wiley, London and New York, 1967
- Moscicki, J., Aharoni, S. M. and Williams, G. *Polymer* 1981, **22**, 571
- Martin, A. J., Meier, G. and Saupe, A. *Faraday Symp.* 1971, **5**, 119
- see for example: Druon, C. and Wachrenier, J. M. *J. de Phys.* 1977, **38**, 47
- Hill, N. E., Vaughan, W. E., Price, A. H. and Davies, M. 'Dielectric Properties and Molecular Behaviour', Reinhold-van Nostrand, London, 1969
- Williams, G. *Adv. Polym. Sci.* 1979, **33**, 60
- Warchol, M. P. and Vaughan, W. E. *Adv. Mol. Relaxation Processes* 1978, **13**, 317
- Wang, C. C. and Pecora, R. *J. Chem. Phys.* 1980, **72**, 5333
- Ouano, A. C. and Pecora, R. *Macromolecules* 1980, **13**, 1167
- Ouano, A. C. and Pecora, R. *Macromolecules* 1980, **13**, 1173
- Williams, G. *Chem. Rev.* 1972, **72**, 55
- Williams, G. *Chem. Soc. Rev.* 1973, **7**, 89